

**Effects of solvents on the intrinsic propensity of peptide backbone conformations**

Wenfei Li, Meng Qin, Zuoxiu Tie, and Wei Wang\*

*National Laboratory of Solid State Microstructure, and Department of Physics, Nanjing University, Nanjing 210093, China*

(Received 23 June 2011; revised manuscript received 16 September 2011; published 28 October 2011)

We investigated the effects of solvents on the intrinsic propensity of peptide backbone conformations based on molecular dynamics simulations. The results show that compared with pure water, aqueous urea decreases the helix propensity. In comparison, methanol decreases the polyproline II (PPII) propensity. Such a solvent dependence of the intrinsic propensity of the backbone conformation is correlated with the solvent dependence of the hydration of the backbone groups and the formation probability of the local intrapeptide hydrogen bonds. Aqueous urea which has low ability to stabilize the local intrapeptide hydrogen bonds disfavors the helical conformation. Whereas, methanol which has low ability to hydrate the backbone groups disfavors the polyproline II conformation. In addition, the solvent effects can be further modulated by the side chains of the peptides. The solvent effects of the intrinsic propensity of peptide backbone conformations observed in this work suggest that changing the intrinsic propensity of the protein backbone conformations can partly contribute to the solvent-induced protein structure and dynamics variations. These results will be useful in understanding the solvent dependence of the conformational distributions of the unfolded proteins or peptides (or intrinsically disordered proteins) in which the global tertiary interactions are less important than that in the well-folded proteins.

DOI: [10.1103/PhysRevE.84.041933](https://doi.org/10.1103/PhysRevE.84.041933)

PACS number(s): 87.15.B–, 87.15.A–, 87.15.kr

**I. INTRODUCTION**

The knowledge on the conformational distribution of the unfolded proteins is fundamental for fully understanding the protein folding problem. Previously, it was generally believed that the unfolded state is dominated by random coils [1,2]. In recent years, this opinion was challenged by a variety of spectroscopic probes which showed that the unfolded states of the proteins are dominated by conformations with backbone dihedral angles corresponding to the left-handed polyproline II helix (PPII) [3–11]. Such observation indicates that the backbone structures of the unfolded proteins are less heterogeneous than that previously believed. Following this new view, the protein folding does not initiate from the random conformations. Instead, the folding proceeds from a locally structured unfolded state to a fully structured folded state, namely, relatively small conformational space needs to be sampled during the folding compared with the conventional scenario.

These findings stimulated extensive characterizations of the intrinsic propensity of the protein backbone conformations by employing a variety of experimental techniques, computational simulations, and coil library surveys [7,8,12–28]. For example, Shi and co-workers investigated the PPII propensity for each amino acid, and found that the propensity scale of PPII is correlated negatively with that of the  $\beta$  sheet for the model peptide AcGGXGGNH<sub>2</sub> (where X stands for any amino acid except for the glycine and proline) by measuring the coupling constant of the backbone amides [7]. In Ref. [13], based on atomistic molecular dynamics simulations, García investigated the conformations of a polyalanine peptide, and found that the polyalanine peptide is dominated by PPII structure. Particularly, a delocalized water channel around the PPII helix was identified and suggested to play a major role in

stabilizing the PPII helix. These works unambiguously support the high PPII preference of the residues in unfolded protein and peptide, and revealed that the hydration of the backbone groups plays a crucial role in stabilizing the PPII.

Since the unfolded state of protein is usually prepared by changing the solvent conditions (e.g., by increasing temperature, adding denaturing cosolvents, adding organic solvents, and changing pH values, etc.), it will be valuable to investigate the solvent dependence of the conformational preference for the peptide in the unfolded state. Meanwhile, as the protein folding and other functional motions are often accompanied with the variations of the local solvent environment, knowledge of the solvent dependence of the conformational preference is also crucial for understanding the molecular mechanisms of protein folding and functional motions. However, compared with its significant biological importance, detailed characterization of the solvent dependence of the protein conformational preference in the unfolded state is very rare. In Ref. [18], Liu and co-workers investigated the solvent dependence of the PPII conformation for model peptides AcGGAGGNH<sub>2</sub> and AcO<sub>2</sub>A<sub>7</sub>O<sub>2</sub>NH<sub>2</sub> using circular dichroism (CD) spectroscopy. Interestingly, by comparing the PPII contents in a number of aliphatic alcohols and water, they found that the PPII content is well correlated with the polarity of the solvents. The solvent with less polarity shows a trend to destabilize the PPII compared with water. In Ref. [28], Whittington and co-workers investigated the effect of urea on the peptide conformations and observed that the urea can increase the CD band around 220 nm. These experimental works provide valuable information on the solvent dependence of the peptide backbone conformations which was considered to be especially important in the initial stage of the protein folding [29]. However, a comprehensive understanding of the effects of solvents on the intrinsic propensity of peptide backbone conformations and its molecular mechanism is still lacking, and further simulation works as complements to these experimental achievements will be highly useful.

\*wangwei@nju.edu.cn

In this work, based on the replica-exchange molecular dynamics simulations, we investigated the relative populations of the major conformational states in water, methanol, and aqueous urea for a model peptide AcGGAGGNH<sub>2</sub>. For this model peptide, the side-chain effects and the global tertiary interactions are largely alleviated. Therefore, it is an ideal model system to investigate the intrinsic propensity of the backbone conformations and is frequently used in experiments to characterize the structural features of unfolded proteins [5,7,16,18,24]. Our results show that compared with water, aqueous urea increases the population of  $\beta$ -strand and decreases the population of helix, but does not affect the population of PPII. In comparison, methanol decreases the population of PPII and increases the population of  $\beta$ -strand, but keeps the helix population unchanged. Such a solvent dependence of the conformational preference largely results from the interplay between the solvent dependence of the backbone hydration and the solvent dependence of the formation probability of the local intrapeptide hydrogen bonds.

## II. METHODS

In this work, the simulations were performed using the AMBER molecular dynamics simulation package with the solvent molecules being treated explicitly [30]. The standard AMBER FF03 force field was used [31,32]. The simulation started from the extended state of the AcGGAGGNH<sub>2</sub> peptide. The peptide was solvated in a solvent box of  $\sim 37000 \text{ \AA}^3$ . Three kinds of solvents (i.e., TIP3P water [33], methanol, and urea of 8 M), were used. To alleviate the boundary effects, the periodic boundary conditions were applied. In treating the long-range electrostatic interactions, the particle mesh Ewald (PME) summation algorithm was employed [34]. A cutoff of  $8.0 \text{ \AA}$  was used for the construction of the nonbonded list. The covalent bonds involving hydrogen atoms were constrained with the SHAKE algorithm [35] and the time step of  $0.002 \text{ ps}$  was used. The extended structure of the peptide was heated to  $1000 \text{ K}$  for  $1.0 \text{ ns}$ . The resulting structures were used as the initial structures for further simulations. The replica exchange molecular dynamics (REMD), which has been widely used in the studying of protein folding and aggregation [36–42], was employed for the conformational sampling. With this method, the peptide at low temperatures has the ability to overcome high energy barriers by being switched to high temperatures, and it provides improved sampling at lower temperatures than standard MD. Further details of the REMD method can be found in Refs. [36,37]. In the REMD simulations, 32 noninteracting replicas with temperatures ranging from  $279.2$  to  $479.2 \text{ K}$  ( $279.2, 283.4, 287.7, 292.1, 296.6, 301.2, 305.9, 310.7, 315.6, 320.6, 325.7, 331.0, 336.3, 341.8, 347.5, 353.3, 359.2, 356.3, 371.6, 378.0, 384.6, 391.4, 398.5, 405.7, 413.1, 420.9, 428.8, 437.1, 447.2, 459.1, 463.2, \text{ and } 479.2 \text{ K}$ ) were conducted simultaneously in parallel. The temperatures were basically distributed exponentially and assigned following the way described in Ref. [43]. Some temperatures were slightly adjusted manually. In REMD simulations, one important parameter is the time interval of the exchange attempt. In literature, very different time intervals ranging from  $\sim 10.0 \text{ fs}$  to  $\sim 20.0 \text{ ps}$  have been used [44–46]. For example, in Ref. [45], a time interval of  $1.0 \text{ ps}$  was suggested to be appropriate

for a 21-residue peptide they studied, whereas, Ref. [44] recommended making the exchange attempt every few time steps. In this work, the time interval of the exchange attempt is  $2.0 \text{ ps}$ . With the above temperature distribution and the time interval of the exchange attempt, we can achieve reasonable sampling quality for the model peptides studied in this work. As a demonstration, Fig. S1 of the Supplemental Material [47] shows the dihedral angle  $\Phi$  and  $\Psi$  of the central alanine, as well as the temperature as a function of simulation time for one of the 32 replicas. We can see that the trajectory frequently hops between different major basins in the  $\Phi$  and  $\Psi$  space, and visits a wide range of temperatures. Such frequent transitions between major states and the visiting of a wide temperature range are essential for the convergence of the REMD simulations. During the REMD simulations, the atomic coordinates were recorded every  $1.0 \text{ ps}$  for further analysis. Totally,  $\sim 50.0 \text{ ns}$  were simulated for each of the 32 replicas. The configurations after the first  $5.0 \text{ ns}$  of each replica were used for analysis. To further investigate the effects of side chains, we also conducted the same simulations for another two model systems, AcGGLGGNH<sub>2</sub> and AcGGDGGNH<sub>2</sub>, which have typical hydrophobic side chain and charged side chain, respectively.

The conformational state was assigned based on the dihedral angles of the central residue. The conformation is defined as PPII,  $\beta$ -strand, and helix when the dihedral angles satisfy the constrains of  $(-125^\circ < \phi < 0^\circ; \psi > 75^\circ \text{ or } \psi < -125^\circ)$ ,  $(\phi < -125^\circ; \psi > 75^\circ \text{ or } \psi < -125^\circ)$  and  $(-125^\circ < \phi < 0^\circ; -75^\circ < \psi < 25^\circ)$ , respectively. A hydrogen bond is formed when the distance between the donor and acceptor is less than  $3.5 \text{ \AA}$ , and the angle formed by donor-hydrogen-acceptor atoms is larger than  $120.0^\circ$ .

## III. RESULTS AND DISCUSSIONS

### A. PPII is one of the major conformations of the model peptide

Figure 1 shows the free-energy landscape projected onto the  $\Phi$  and  $\Psi$  dihedral angles at  $279.2 \text{ K}$  (a) and  $479.2 \text{ K}$  (b) in water. One can see that there are three major states being largely populated at both temperatures. These states correspond to the helix (basin A), PPII (basin B), and  $\beta$ -strand (basin C), respectively. The significant population of the PPII supports the experimental observation that the PPII has a major contribution to the unfolded state of peptide [3–11]. The populations of the three major states rely on the temperature

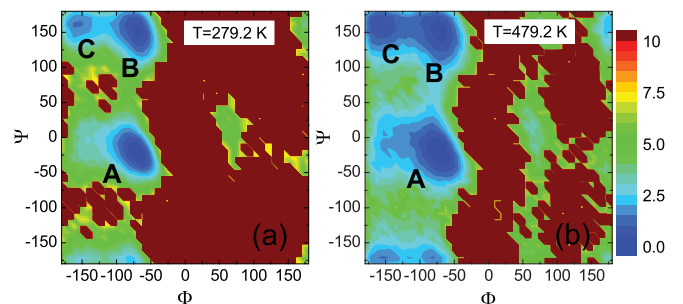


FIG. 1. (Color online) Free-energy landscape projected onto the  $\Phi$  and  $\Psi$  angles at  $279.2 \text{ K}$  (a) and  $479.2 \text{ K}$  (b). The unit of free energy is  $k_B T$ .

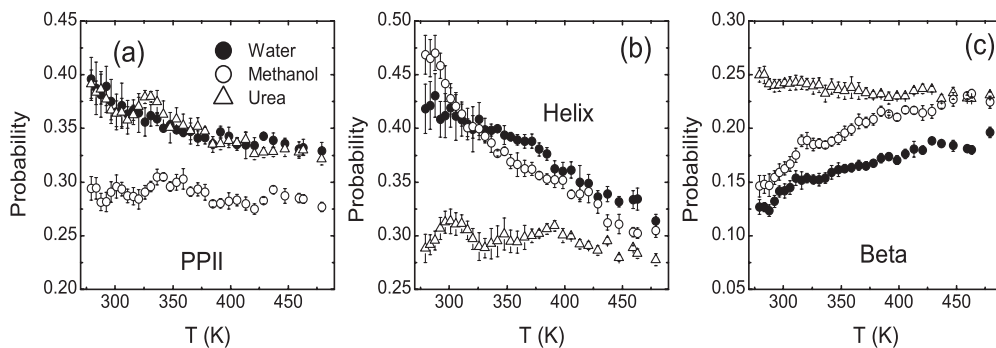


FIG. 2. Populations of the PPII (a), helix (b), and  $\beta$ -strand (c) as a function of temperature in water (solid circle), methanol (open circle), and aqueous urea (open triangle).

strongly. Compared with the low-temperature case, both the PPII and helix contents are decreased at high temperature. In comparison, the content of the  $\beta$ -strand is increased, suggesting that the high temperature tends to increase the relative stability of the  $\beta$ -strand. Such observation is consistent with the simulation results of Garca for a polyalanine peptide [13]. Other experimental works also observed that increasing the temperature can increase the  $\beta$ -strand content of the unfolded proteins [6,48].

### B. Solvent effects on the conformational propensity

To investigate the effect of solvent on the conformational propensity of the peptide, we calculated the populations of the three major states for typical solvents, namely, water, aqueous urea (typical denaturing cosolvent), and methanol (typical organic solvent). Here, the assignment of the three major conformational states was based on the constraints described in the Methods section. However, other conformations beyond the above constraints can also be observed, therefore, the sum of the populations of the three major states is less than unity. Figure 2 shows the populations of the PPII (a), helix (b), and  $\beta$ -strand (c) as a function of temperatures in water (solid circle), methanol (open circle), and aqueous urea (open triangle). The error bars were added to show the convergence of the simulations. In estimating the errors of the calculated distributions, we divided the full-length data (the data of the first 5.0 ns were excluded) into five time windows equally and calculated the populations of the secondary structures for each time window. The error bars are represented by the standard error from the results of the five time windows. The relative small error bars suggest reasonable convergence of the REMD simulations. It is worth mentioning that in this work the conformational states were assigned based purely on the conformations as described in the previous section, and the sharp boundaries used in the conformation assignment may contribute to the errors in Fig. 2. Recently, a more sophisticated assignment method which combines the trajectory history and the conformations was proposed, and can improve the conformation assignment significantly [49,50]. One can see that compared with water, methanol significantly decreases the population of the PPII, and increases the population of the  $\beta$ -strand (see the differences between the populations in methanol and in water), but does not change the population of the helix. In comparison, urea significantly decreases the

population of the helix, and increases the population of the  $\beta$ -strand, but does not change the population of the PPII. In Ref. [18], Liu and co-workers observed that the organic solvent methanol, ethanol, and isopropanol can decrease the PPII content dramatically. The present result is consistent with such observation.

The above results suggest that both methanol and aqueous urea can affect the conformational distribution of the model peptide dramatically. In literature, people found that the propensity scale of the PPII is well anticorrelated with that of the  $\beta$ -sheet [7]. Therefore, it is interesting to calculate the relative stability of the PPII and  $\beta$ -strand based on the simulation data. Figure 3 shows the free-energy difference between the  $\beta$ -strand and PPII, which is calculated by  $\Delta F = -k_B T \ln[P(\beta)/P(\text{PPII})]$ . The error bars were obtained with the same method as that in Fig. 2. Here, the  $P(\beta)$  and  $P(\text{PPII})$  are the probability of the  $\beta$ -strand and PPII, respectively, sampled by the central alanine, and the  $k_B$  is the Boltzmann constant. From Fig. 3 we can see that both methanol and aqueous urea decrease the relative free energy with nearly the same magnitude, namely, the PPII is destabilized relative to the

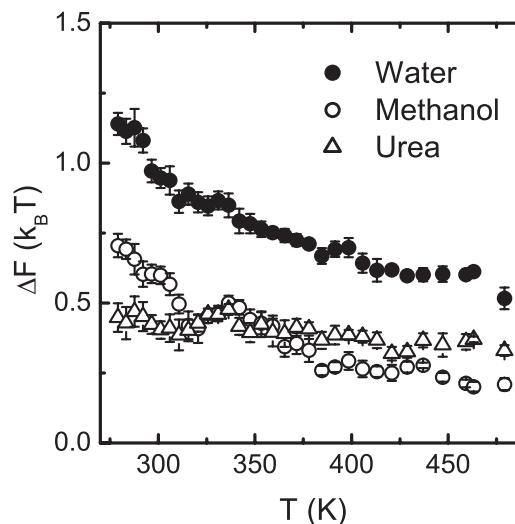


FIG. 3. Free-energy difference between the PPII and  $\beta$ -strand as a function of temperature in water (solid circle), methanol (open circle), and aqueous urea (open triangle). The unit of free-energy difference is  $k_B T$ .

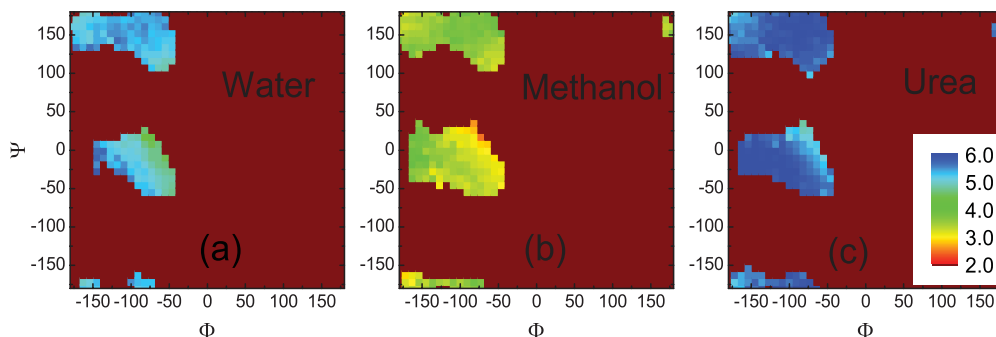


FIG. 4. (Color online) Total number of hydrogen bonds formed between the backbone groups and the water (a), methanol (b), and aqueous urea (c) at different regions of the dihedral angle space at the temperature of 301.2 K. The backbone groups around the central alanine, namely, the CO of the Gly2 and Ala3, and the NH of the Ala3 and Gly4, were included in counting the hydrogen bonds. For maintaining reasonable statistics, the hydration data of the conformations with populations less than 0.001 are not shown (represented by the background with wine color).

$\beta$ -strand. However, from Fig. 2, the decreasing mechanism of the relative free energy is quite different. The decreasing of the relative free energy by methanol results from the simultaneous decreasing of the PPII content and the increasing of the  $\beta$ -strand content. In comparison, the decreasing of the relative free energy by urea mainly results from the increasing of the  $\beta$ -strand content, which is accompanied by the decreasing of the helical conformation.

### C. Mechanism of the solvent dependence of the conformational propensity

In literature, a number of simulations and coil library surveys showed that the solvation of the backbone plays a major role in stabilizing the PPII [14–16,51,52]. Meanwhile, the modulation of the backbone solvation by the side chain can result in sequence dependence of the PPII propensity [16]. For example, based on Monte Carlo simulations, Mezei and co-workers found that there are more hydrogen-bonded water molecules around both NH and CO groups in PPII than in  $\beta$ -strand and  $\alpha$  helix [21]. On the other hand, it is well believed that the helical conformation is stabilized by the local intrapeptide hydrogen bonds. Investigating the detailed stabilization mechanisms of the secondary structures is beyond the scope of this paper. Here, we try to understand the above-observed solvent dependence of the conformational propensity of the model peptide on the basis of the hydration of the backbone groups and the local intrapeptide hydrogen bond formation. Figure 4 shows the total number of hydrogen bonds formed between the backbone groups around the central alanine and solvent molecules at different regions of the dihedral angle space averaged over the sampled structures at the temperature of 301.2 K. The backbone CO and NH around the central alanine, namely, the CO of the Gly2 and Ala3, and the NH of the Ala3 and Gly4 are included in counting the hydrogen bonds. One can see that methanol forms much fewer hydrogen bonds with the backbone groups compared to water solvent. In comparison, the hydrogen bonds formed between the aqueous urea (including the water and urea molecules) and backbone groups only increases slightly compared to the water. Such solvent dependence of the backbone hydration correlates well with the solvent dependence of the PPII content observed

in Fig. 2(a), which in turn supports the previous suggestions that backbone hydration is important for the stabilization of the PPII conformation [14–16,51,52]. The correlation between the populations of the PPII and the number of hydrogen bonds is demonstrated more directly in Fig. S2 of the Supplemental Material [47], which shows the correlation plots between the populations of the PPII and the number of hydrogen bonds at different temperatures for each of the three solvents and the correlation plots for the three solvents at the same temperatures.

To further understand the effect of solvent on the conformational propensity of the model peptide, we calculated the probabilities of the intrapeptide hydrogen bonds between the backbone groups of the model peptide. The results are presented in Fig. 5. One can see that methanol has a very weak effect on the formation probabilities of the intrapeptide hydrogen bonds at 301.2 K as shown in Figs. 5(a)–5(c). In comparison, urea decreases the formation probability of the intrapeptide hydrogen bonds dramatically. Particularly, formation probabilities of the hydrogen bonds between the NH of the Gly5 (Gly4) and the CO of the Gly2 (Gly1) are significantly decreased by the addition of the aqueous urea. Similar results are observed for higher temperatures, but the effects are relatively weaker as shown in Figs. 5(d)–5(i). These results suggest that the destabilization of the helical conformation by aqueous urea observed in Fig. 2 largely results from the decreasing of the local intrapeptide hydrogen bonds since the local intrapeptide hydrogen bonds are the main driving force for the stabilization of the helical conformation. Here, the helical conformation is calculated only on the basis of dihedral angles. It may include both the helical and turn structures. Figure 5 also suggests that higher temperatures tend to destabilize the  $(i, i + 3)$  hydrogen bonds, and slightly increase the populations of the  $(i, i + 2)$  hydrogen bonds.

There are at least two possible mechanisms by which the solvents alter the formation probability of the local intrapeptide backbone hydrogen bonds. One possible mechanism is the competition between the solvent-peptide hydrogen bonds and the intrapeptide hydrogen bonds. For example, the hydration of the backbone groups will decrease the formation probability of the intrapeptide hydrogen bonds since the donors or acceptors are occupied by the solvent groups.

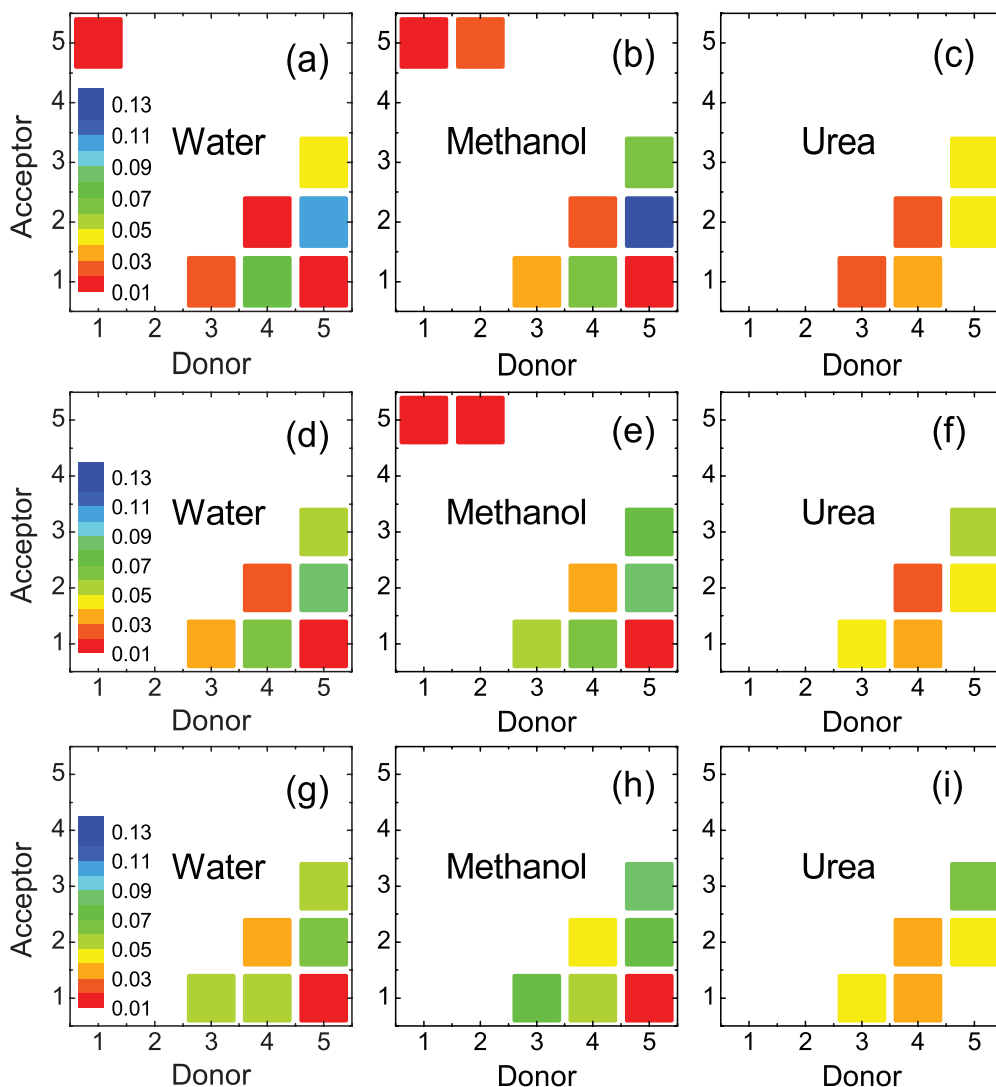


FIG. 5. (Color online) The probability for the formation of the local intrapeptide hydrogen bonds between the backbone groups in water (left panels), methanol (middle panels), and aqueous urea (right panels) at 301.2 K (a)–(c), 353.3 K (d)–(f), and 405.7 K (g)–(i).

Another mechanism is the direct interaction between the hydrogen-bonded solvent molecules and the peptide atoms. Here, the hydrogen-bonded solvent molecules refer to the solvent molecules which form hydrogen bonds with the peptide backbone groups. From Fig. 4, the backbone groups are only slightly more hydrated in aqueous urea than those in water. Therefore, the observed decreasing of the intrapeptide hydrogen bonds by urea most likely results from the direct interactions between the hydrogen-bonded urea molecules and the peptide atoms. Since the urea molecule has a much larger size than the water molecule, the steric repulsion and dispersion interaction between the hydrogen-bonded urea molecule and the peptide atoms is stronger than that between water and peptide atoms. For example, the stronger steric blocking effect due to the large size of the hydrogen-bonded urea molecule tends to prevent the freely approaching of other peptide atoms to the hydrogen bond donors and acceptors adjacent to the urea bonded backbone groups. On the other hand, the stronger dispersion interaction tends to arrest the approaching peptide atoms, and therefore reduce the hydrogen

bonding probability of the nearby hydrogen bond donors and acceptors. To manifest the importance of such blocking and dispersion effects of the urea molecules on the local intrapeptide hydrogen bond formation, we performed three simulations. In two of the simulations, one water molecule and one urea molecule were hydrogen bonded to the NH group of the central alanine, respectively, by imposing distance and angle restraints. As a control, another simulation in which the backbone groups were not hydrogen bonded to any solvent molecule, was performed. To eliminate other possible effects, the simulations were conducted in vacuum and with electrostatic interactions switched off. Therefore, the differences between these simulations mainly result from the different steric blocking and dispersion interactions by the hydrogen-bonded solvent molecules. Due to the small number of atoms in the model systems, the conventional molecular dynamics were used, and the simulations were conducted at 300, 320, 340, 360, and 380 K. It is worth noting that the sampled conformations and the absolute values of the calculated quantities are unrealistic due to the simplifications

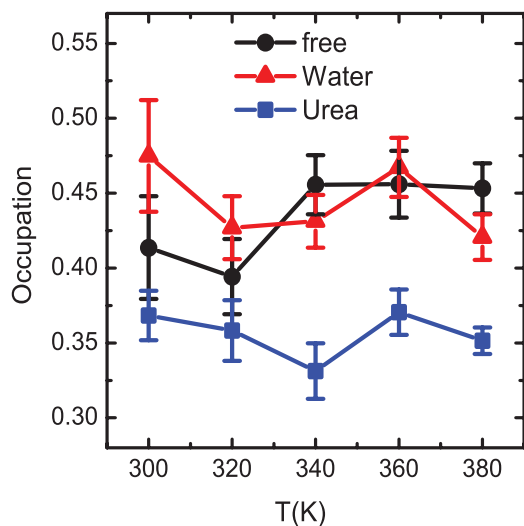


FIG. 6. (Color online) Occupation number of the heavy atoms around the backbone O of the central alanine with the backbone N of the Ala3 hydrogen bonded by one urea molecule (square) or one water molecule (triangle). For comparison, the result for free peptide is also shown (solid circle). The error bars were calculated by blocking average with time windows of 0.5 ns, and represent the standard error. The total simulation time for each case is 10.0 ns.

made above. However, the differences between the simulations can unambiguously identify the contributions of the steric blocking and dispersion effects arising from the hydrogen-bonded molecules.

In Fig. 6, we compared the averaged occupation number of the backbone O of the central alanine (i.e., the number of heavy atoms which are within 3.5 Å from the backbone O of the alanine. The neighboring heavy atoms, namely, the heavy atoms in Ala3 and Gly4 are not considered). This hydrogen bond acceptor (i.e., backbone O of the alanine) is quite close to the hydrogen-bonded backbone NH, therefore its hydrogen bonding ability is easier to be affected by the hydrogen-bonded solvent molecules. One can see that the occupation number is much smaller for the urea bonded peptide than those for the water bonded peptide and the free peptide. In comparison, the occupation numbers for the later two peptides are quite similar. These results suggest that compared with the water molecule, the steric blocking and dispersion interaction between the urea and the peptide atoms can partly prevent the peptide atoms from approaching the nearby hydrogen bond acceptors and donors, therefore decrease the formation probability of intrapeptide backbone hydrogen bonds. Such result has valuable implication for the urea-induced unfolding mechanism of proteins. Recently, there are continuing debates about the denaturing mechanism of the urea [53–58]. Particularly, recent experimental work suggested that the urea destabilizes proteins by hydrogen bonding to the peptide groups [59]. Our present results show that once the urea molecule is hydrogen bonded to the backbone groups, the strong steric blocking and dispersion interactions resulted from its large size can partly hinder the formation of the intrapeptide hydrogen bonds, and therefore changes the intrinsic propensity of the backbone conformation. Such alteration of the intrinsic propensity of

the protein backbone conformations by urea may contribute to the urea-induced denaturation of proteins.

In addition to the steric blocking and dispersion effects discussed above, other factors (e.g., urea-induced electrostatic interactions and the entropy change of the solvent) may also affect the formation probability of the intrapeptide hydrogen bonds, which is difficult to analyze based only on the simulation results of this work.

#### D. Side-chain modulations to the solvent dependence of the conformational propensity

In the above discussions, we focus on the model system AcGGAGGNH<sub>2</sub> since the alanine represents the common part of all the amino acids except for glycine and proline. Therefore, the effects of solvent on the conformational distributions of the AcGGAGGNH<sub>2</sub> represent the effects of solvent on the intrinsic propensity of the backbone conformation. However, the conformational distributions of the realistic amino acid chains may also depend on the identities of the side chain and other long-range global interactions. As a demonstration of the possible modulations of the solvent effects by side chains, Fig. 7 shows the conformational distributions of two representative model peptides, AcGGLGGNH<sub>2</sub> and AcGGDGGNH<sub>2</sub>, which have a typical hydrophobic side chain and charged side chain, respectively. We can see that the side chain of the central leucine has relatively weak effects on the solvent effects. Both the populations of the PPII and helix are changed by the solvents with similar trends as those of the model system AcGGAGGNH<sub>2</sub>, except that the effects of the solvents on the  $\beta$ -strand becomes relatively weaker. For example, the aqueous urea does not change the population of the PPII, but decreases the population of the helix. Similarly, the methanol does not change the population of the helix, but decreases the population of the PPII. In addition, the probability of the local intrapeptide hydrogen bonds and the hydrogen bonds between the solvent and backbone groups are also similar to those of the AcGGAGGNH<sub>2</sub> as shown in Figs. S3 and S4 in the Supplemental Material [47]. In comparison, the side chain of the central aspartic acid strongly affects the solvent effects. Compared with the AcGGAGGNH<sub>2</sub>, the methanol dramatically increases the population of the PPII and decreases the population of the helix, although the probability of the hydrogen bonds between the solvent and backbone groups are not changed by the side chain as shown in Fig. S3. Figure S4 also shows that the formation probability of the local intrapeptide hydrogen bonds in methanol is reduced.

More detailed investigations show that for the AcGGDGGNH<sub>2</sub>, the charged side chain of the central aspartic acid has high ability to form hydrogen bonds with the backbone groups. According to previous studies [60,61], such hydrogen bonds between the side chain and the backbone groups of the nearby residues can greatly contribute to the stability of the PPII conformation due to the geometrical constraints (Note that we used a much looser definition of the PPII than in Refs. [60,61]). Figure 8(a) shows the probability for the formation of the hydrogen bonds between the backbone NH groups and the side chain of the central aspartic acid in water, methanol, and aqueous urea at 301.2 K. We can see that the

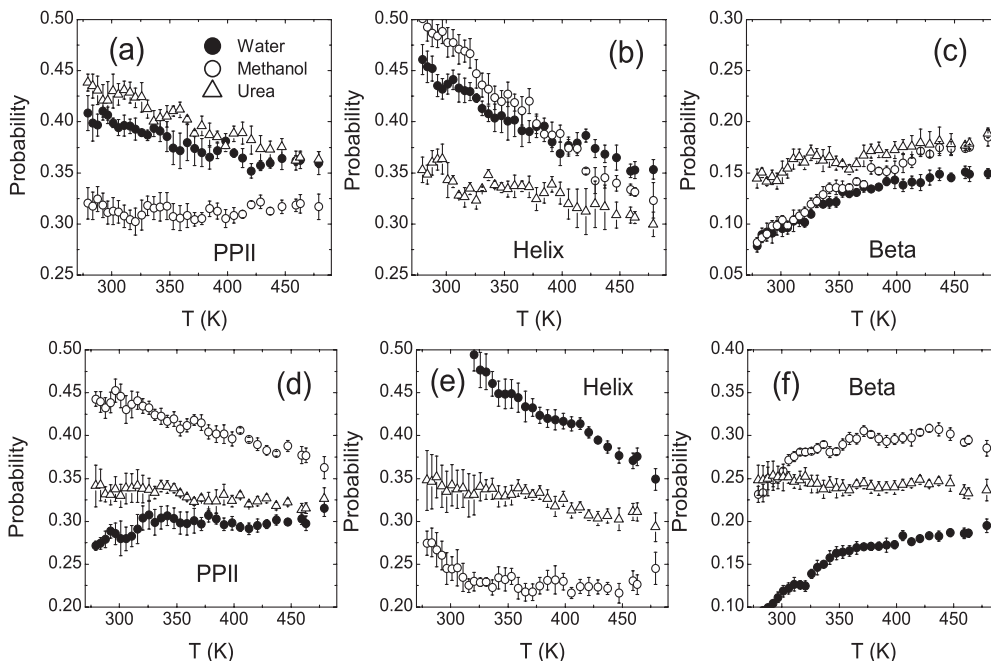


FIG. 7. Populations of the PPII (a) and (d), helix (b) and (e), and  $\beta$ -strand (c) and (f) as a function of temperature in water (solid circle), methanol (open circle), and aqueous urea (open triangle) for AcGGLGGNH<sub>2</sub> (upper) and AcGGDGGNH<sub>2</sub> (lower).

formation probability of the hydrogen bonds between the side chain of the aspartic acid and the backbone groups of the next two residues is much higher in methanol than that in water and aqueous urea. Figure 8(b) shows the ratios of the secondary structure populations with and without side chain-backbone hydrogen bonds for methanol at different temperatures. A larger ratio ( $>1.0$ ) indicates that the side chain-backbone hydrogen bonds stabilize the secondary structure. Similarly, a smaller ratio ( $<1.0$ ) indicates that the side chain-backbone hydrogen bonds destabilize the secondary structure. We can see that the side chain-backbone hydrogen bonds highly stabilize the PPII and  $\beta$ -strand conformation, and destabilize

the helical conformation, which contributes to the high PPII and  $\beta$ -strand populations and the low helix population for methanol observed in Fig. 7.

The above results show that methanol and aqueous urea can change the intrinsic propensity of the backbone conformations to a large extent. Such solvent effects of the intrinsic propensity of the backbone conformations can be further modulated by the side chains. Particularly, different side chains can modulate such solvent effects by different extent and mechanisms. Therefore, to fully understand the effects of solvent on the conformational propensity of a certain amino acid chain, more detailed work to characterize the effects of side-chain identities on the conformational propensity and its mechanism are needed.

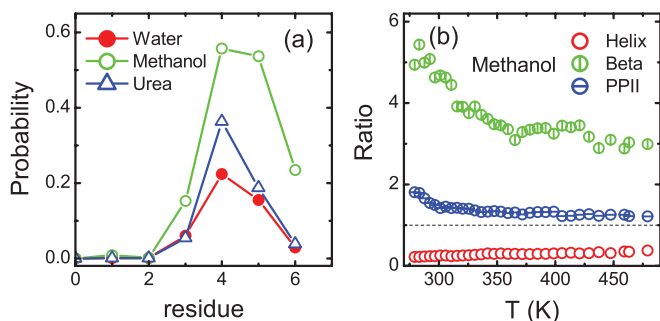


FIG. 8. (Color online) (a) The probability for the formation of the hydrogen bonds between the side chain of the central aspartic acid and the backbone groups of the peptide in water, methanol, and aqueous urea at 301.2 K. (b) Ratio of the secondary structure populations with and without side chain-backbone hydrogen bonds in methanol as a function of temperature. The NH groups of the Gly4 and Gly5 were included as the hydrogen bond donors in panel (b). Considering possible distortions of the hydrogen bond geometry by side-chain rigidity, a looser cutoff ( $90.0^\circ$ ) for the donor-hydrogen-acceptor angle was used in both (a) and (b). The dash line represents the ratio of unity.

#### IV. SUMMARY

Many biological processes (i.e., protein folding, translocation, etc.) involve the variation of the local solvent environment. In this work, by employing the REMD simulations, we investigated the effects of solvents on the conformational distributions of the model peptide AcGGAGGNH<sub>2</sub> at wide temperature range. Our results provide a detailed characterization of the solvent dependence of the intrinsic propensity of the peptide backbone conformations, and its underlying molecular mechanisms. Particularly, we revealed that the solvent dependence of the intrinsic propensity of the protein backbone conformation largely results from the interplay between the solvent dependence of the backbone hydration and the solvent dependence of the local intrapeptide hydrogen bond formation, and can be further modulated by the side chains. In addition, our results suggest that changing the intrinsic propensity of the backbone local conformation by the hydrogen-bonded urea molecules may play a crucial role on the urea-induced protein denaturation.

It is worth emphasizing that there are a number of factors which can contribute to the solvent-induced conformational changes of proteins in addition to the above-observed variations of the intrinsic propensity of backbone conformations, including the side-chain modulations and other long-range global interactions. Therefore, for realistic proteins, the contribution of the solvent effects on the intrinsic propensity of the protein backbone conformations may be buried by other more complicated factors. For example, in a recent work by Canchi and co-workers [62], the urea-induced unfolding of a designed protein Trp-cage was simulated by REMD. Their results showed that the backbone of the protein only slightly more hydrated in the unfolded state than that in the folded state. Based on the above observations, the authors concluded that the hydrogen bonding of urea to the peptide backbone does not play a dominant role in the denaturation of the Trp-cage. We speculate that the solvent effects on the intrinsic propensity of the backbone conformation are more important for the conformational distributions of the unfolded proteins or intrinsically disordered proteins in which the long-range global interactions are less important than those in the well-folded proteins.

In this work, the AMBER FF03 force field was used. The absolute values of the peptide conformational populations extracted from the molecular dynamics simulations may depend on the used force fields. For example, in Refs. [63,64], the authors investigated the force-field dependence of the conformational populations of peptides for a number of current

force fields, and showed that most force fields, including the AMBER FF03 force field used in this work, do overpopulate the  $\alpha$ -helical region. However, in the present work, the variation of the conformational population induced by changing the solvent is more relevant to the major conclusions, which is less dependent on the specific force field used. Undoubtedly, more detailed work using a number of different force fields will be highly useful in understanding the solvent effects of the intrinsic propensity of the backbone conformations. In addition, the discussions in this work mostly based on the simulation results of the model peptide AcGGAGGNH<sub>2</sub> which fully eliminates the effects of the side-chain interactions, and on two peptides with a typical hydrophobic side chain and charged side chain, respectively. To further study the side-chain effects on the backbone conformational propensity, other peptides involving different side chains and neighboring residues are needed.

#### ACKNOWLEDGMENTS

The authors thank the Shanghai Supercomputer Center and High Performance Computing Center of Nanjing University for the computational support. This work was supported by the National Natural Science Foundation of China (Grants No. 10704033, No. 11174134, No. 10834002, and No. 10974088), Natural Science Foundation of Jiangsu Province (Grants No. BK2011546 and No. BK2009008), and PAPD.

- 
- [1] C. Tanford, *Adv. Protein Chem.* **23**, 121 (1968).  
 [2] P. J. Flory, *J. Statistical Mechanics of Chain Molecules* (Wiley, New York, 1969).  
 [3] S. Woutersen and P. Hamm, *J. Phys. Chem. B* **104**, 11316 (2000).  
 [4] C. D. Poon *et al.*, *J. Am. Chem. Soc.* **122**, 5642 (2000).  
 [5] Z. Shi *et al.*, *Chem. Rev.* **106**, 1877 (2006).  
 [6] Z. Shi *et al.*, *Proc. Natl. Acad. Sci. USA* **99**, 9190 (2002).  
 [7] Z. Shi *et al.*, *Proc. Natl. Acad. Sci. USA* **102**, 17964 (2005).  
 [8] K. Chen *et al.*, *J. Am. Chem. Soc.* **127**, 10146 (2005).  
 [9] W. G. Han *et al.*, *J. Phys. Chem. B* **102**, 2587 (1998).  
 [10] R. Schweitzer-Stenner *et al.*, *J. Am. Chem. Soc.* **123**, 9628 (2001).  
 [11] A. L. Rucker and T. P. Creamer, *Protein Sci.* **11**, 980 (2002).  
 [12] J. Makowska *et al.*, *Proc. Natl. Acad. Sci. USA* **103**, 1744 (2006).  
 [13] A. E. Garcia, *Polymer* **45**, 669 (2004).  
 [14] F. Avbelj, P. Luo, and R. L. Baldwin, *Proc. Natl. Acad. Sci. USA* **97**, 10786 (2000).  
 [15] F. Avbelj and R. L. Baldwin, *Proc. Natl. Acad. Sci. USA* **101**, 10967 (2004).  
 [16] A. Kentsis, M. Mezei, and R. Osman, *Proteins* **61**, 769 (2005).  
 [17] A. Kentsis *et al.*, *Proteins* **55**, 493 (2004).  
 [18] Z. Liu *et al.*, *J. Am. Chem. Soc.* **126**, 15141 (2004).  
 [19] N. Sreerama and R. W. Woody, *Proteins* **36**, 400 (1999).  
 [20] R. Srinivasan and G. D. Rose, *Proc. Natl. Acad. Sci. USA* **96**, 14258 (1999).  
 [21] M. Mezei *et al.*, *Proteins* **55**, 502 (2004).  
 [22] R. V. Pappu, R. Srinivasan, and G. D. Rose, *Proc. Natl. Acad. Sci. USA* **97**, 12565 (2000).  
 [23] A. N. Drozdov, A. Grossfield, and R. V. Pappu, *J. Am. Chem. Soc.* **126**, 2574 (2004).  
 [24] L. Ding *et al.*, *J. Am. Chem. Soc.* **125**, 8092 (2003).  
 [25] V. Ramakrishnan, R. Ranbhor, and S. Durani, *J. Am. Chem. Soc.* **126**, 16332 (2004).  
 [26] F. Eker *et al.*, *J. Phys. Chem. B* **107**, 358 (2003).  
 [27] J. B. Hamburger *et al.*, *Biochemistry* **43**, 9790 (2004).  
 [28] B. J. Whittington *et al.*, *Biochemistry* **44**, 6269 (2005).  
 [29] G. D. Rose, *Proc. Natl. Acad. Sci. USA* **103**, 16623 (2006).  
 [30] D. A. Case *et al.*, *Computer Code Amber 8* (University of California, San Francisco, 2004).  
 [31] Y. Duan *et al.*, *J. Comp. Chem.* **24**, 1999 (2003).  
 [32] M. C. Lee and Y. Duan, *Proteins* **55**, 620 (2004).  
 [33] W. L. Jorgensen, *et al.*, *J. Chem. Phys.* **79**, 926 (1983).  
 [34] T. Darden, D. York, and L. Pederson, *J. Chem. Phys.* **98**, 10089 (1993).  
 [35] J. P. Ryckaert, G. Cicotti, and H. J. C. Berendsen, *J. Comput. Phys.* **23**, 327 (1993).  
 [36] Y. Sugita and Y. Okamoto, *Chem. Phys. Lett.* **314**, 141 (1999).  
 [37] R. Zhou, *J. Mol. Graphics Modell.* **22**, 451 (2004).  
 [38] A. E. Garcia and K. Y. Sanbonmatsu, *Proteins* **42**, 345 (2001).  
 [39] A. E. Garcia and J. N. Onuchic, *Proc. Natl. Acad. Sci. USA* **100**, 13898 (2003).  
 [40] R. Zhou, B. J. Berne, and R. Germain, *Proc. Natl. Acad. Sci. USA* **98**, 14931 (2001).  
 [41] W. F. Li *et al.*, *Proteins* **67**, 338 (2007).

- [42] W. F. Li *et al.*, *J. Am. Chem. Soc.* **130**, 892 (2008).
- [43] G. H. Zuo *et al.*, *J. Phys. Chem. B* **114**, 5835 (2010).
- [44] D. Sindhikara, Y. Meng Yilin, and A. E. Roitberg, *J. Chem. Phys.* **128**, 024103 (2008).
- [45] W. Zhang, C. Wu, and Y. Duan, *J. Chem. Phys.* **123**, 154105 (2005).
- [46] S. B. Opps and J. Schofield, *Phys. Rev. E* **63**, 056701 (2001).
- [47] See Supplemental Material at <http://link.aps.org/supplemental/10.1103/PhysRevE.84.041933> for Figs. S1, S2, S3, and S4.
- [48] W. Y. Yang, E. Larios, and M. Gruebele, *J. Am. Chem. Soc.* **125**, 16220 (2003).
- [49] G. S. Buchner *et al.*, *BBA-Proteins Proteomics* **1814**, 1001 (2011).
- [50] N. V. Buchete and G. Hummer, *J. Phys. Chem. B* **112**, 6057 (2008).
- [51] F. Eker, K. Griebenow, and R. J. Schweitzer-Stenner, *J. Am. Chem. Soc.* **125**, 8178 (2003).
- [52] M. A. Kelly *et al.*, *Biochemistry* **40**, 14376 (2001).
- [53] A. Wallqvist, D. G. Covell, and D. Thirumalai, *J. Am. Chem. Soc.* **120**, 427 (1998).
- [54] H. Hua *et al.*, *Proc. Natl. Acad. Sci. USA* **105**, 16928 (2008).
- [55] E. O'Brien *et al.*, *J. Am. Chem. Soc.* **129**, 7346 (2007).
- [56] P. Rossky, *Proc. Natl. Acad. Sci. USA* **105**, 16825 (2008).
- [57] B. Bennion and V. Daggett, *Proc. Natl. Acad. Sci. USA* **100**, 5142 (2003).
- [58] D. Klimov, J. Straub, and D. Thirumalai, *Proc. Natl. Acad. Sci. USA* **101**, 14760 (2004).
- [59] W. K. Lim, J. Rosgen, and S. W. Englander, *Proc. Natl. Acad. Sci. USA* **106**, 2595 (2009).
- [60] T. P. Creamer and M. N. Campbell, *Adv. Protein. Chem.* **62**, 263 (2002).
- [61] B. J. Stapley and T. P. Creamer, *Protein Sci.* **8**, 587 (1998).
- [62] D. R. Canchi, D. Paschek, and A. E. García, *J. Am. Chem. Soc.* **132**, 2338 (2010).
- [63] R. B. Best, N. V. Buchete, and G. Hummer, *Biophys. J.* **95**, L07 (2008).
- [64] N. V. Buchete and G. Hummer, *Phys. Rev. E* **77**, 030902 (2008).